Intercalibration of radioisotopic and astrochronologic time scales for the Cenomanian-Turonian boundary interval, Western Interior Basin, USA

Stephen R. Meyers[1]*, Sarah E. Siewert[1], Brad S. Singer[1], Bradley B. Sageman[2], Daniel J. Condon[3], John D. Obradovich[4], Brian R. Jicha[1], and David A. Sawyer[4]

[1]Department of Geoscience, University of Wisconsin–Madison, 1215 West Dayton Street, Madison, Wisconsin 53706, USA
[2]Department of Earth and Planetary Sciences, Northwestern University, 1850 Campus Drive, Evanston, Illinois 60208, USA
[3]NERC (Natural Environment Research Council) Isotope Geoscience Laboratory, British Geological Survey, Keyworth NG12 5GG, UK
[4]U.S. Geological Survey, MS 980, Denver, Colorado 80225, USA

ABSTRACT

We develop an intercalibrated astrochronologic and radioisotopic time scale for the Cenomanian-Turonian boundary (CTB) interval near the Global Stratotype Section and Point in Colorado, USA, where orbitally influenced rhythmic strata host bentonites that contain sanidine and zircon suitable for $^{40}Ar/^{39}Ar$ and U-Pb dating. Paired $^{40}Ar/^{39}Ar$ and U-Pb ages are determined from four bentonites that span the *Vascoceras diartianum* to *Pseudaspidoceras flexuosum* ammonite biozones, utilizing both newly collected material and legacy sanidine samples of J. Obradovich. Comparison of the $^{40}Ar/^{39}Ar$ and U-Pb results underscores the strengths and limitations of each system, and supports an astronomically calibrated Fish Canyon sanidine standard age of 28.201 Ma. The radioisotopic data and published astrochronology are employed to develop a new CTB time scale, using two statistical approaches: (1) a simple integration that yields a CTB age of 93.89 ± 0.14 Ma (2σ; total radioisotopic uncertainty), and (2) a Bayesian intercalibration that explicitly accounts for orbital time scale uncertainty, and yields a CTB age of 93.90 ± 0.15 Ma (95% credible interval; total radioisotopic and orbital time scale uncertainty). Both approaches firmly anchor the floating orbital time scale, and the Bayesian technique yields astronomically recalibrated radioisotopic ages for individual bentonites, with analytical uncertainties at the permil level of resolution, and total uncertainties below 2‰. Using our new results, the duration between the Cenomanian-Turonian and the Cretaceous-Paleogene boundaries is 27.94 ± 0.16 Ma, with an uncertainty of less than one-half of a long eccentricity cycle.

INTRODUCTION

Recent advances in radioisotopic dating and astrochronology, and their intercalibration (Kuiper et al., 2008), potentially provide unprecedented accuracy and precision in the measurement of geologic time. For example, chemical abrasion (CA) (Mattinson, 2005) and ultra low-blank, isotope-dilution thermal-ionization mass spectrometry (ID-TIMS) for U-Pb zircon geochronology now enables ages to be determined from individual zircons to better than ±2‰ (total radioisotopic uncertainty; including analytical, tracer solution, and decay constant sources) for the entire Phanerozoic (e.g., Mundil et al., 2004; Crowley et al., 2007; Schoene et al., 2010). In parallel, an astronomically calibrated age of 28.201 ± 0.046 Ma (2σ) for the $^{40}Ar/^{39}Ar$ neutron fluence standard Fish Canyon sanidine may improve the total uncertainty of this method to ~3‰ (Kuiper et al., 2008). In this study, these advances serve as a springboard to develop a new high-resolution intercalibrated $^{40}Ar/^{39}Ar$, U-Pb, and astrochronologic time scale for the Cenomanian-Turonian boundary (CTB) interval near the Global Boundary Stratotype Section and Point (GSSP) in Colorado, where orbitally influenced rhythmic strata (Sageman et al., 1997; Meyers et al., 2001) host bentonites that contain sanidine and zircon suitable for dating. This provides a rare opportunity to directly intercalibrate two independent radioisotopic chronometers against an astrochronologic age model (Meyers et al., 2001; Sageman et al., 2006), and in doing so, allows for testing the astronomically calibrated Fish Canyon sanidine age proposed by Kuiper et al. (2008). We consider three fundamental sources of uncertainty associated with the radioisotopic ages (analytical, tracer solution or age of neutron fluence standard, and decay constants), as well as uncertainties in the astrochronology.

To develop the new CTB time scale we have determined paired $^{40}Ar/^{39}Ar$ and U-Pb ages from four bentonites spanning the *Vascoceras diartianum* to *Pseudaspidoceras flexuosum* ammonite biozones. These analyses employ both newly collected material and legacy sanidine samples of Obradovich (1993), which provide a direct link to the existing Cretaceous time scale (Gradstein et al., 2004). For two bentonites (*Watinoceras devonense* and *Neocardioceras juddii* zones), material has been analyzed from multiple locations throughout the Western Interior Basin, which allows an assessment of the temporal correlation of individual bentonites from the perspective of both sanidine and zircon.

A critical step in the comparison of these results is the selection of a Fish Canyon sanidine age, so we investigate a range of proposed values, and consider the implications of each for the consistency of the $^{40}Ar/^{39}Ar$ and U-Pb ages. Following the identification of an optimal Fish Canyon sanidine age, we use a new statistical methodology to combine the radioisotopic and astrochronologic data, anchoring the floating orbital time scale, and yielding astronomically recalibrated radioisotopic ages for individual bentonites with greatly reduced uncertainties.

STRATIGRAPHY AND SAMPLING

Bentonites were sampled from four localities (Item DR1 in the GSA Data Repository[1]): (1) Lohali Point, Arizona (Kirkland, 1991), (2) Thayer County, Nebraska (Elder, 1987), (3) Red Wash, New Mexico (Elder, 1991), and (4) the GSSP near Pueblo, Colorado (Kennedy et al., 2005). Legacy samples of sanidine from Obradovich (1993) were available from the bentonites in Arizona, Nebraska, and New Mexico that, based on revised biostratigraphy (Kennedy et al., 2005; Cobban et al., 2006), occur within the *V. diartianum* (90-O-30), *Euomphaloceras septemseriatum* (90-O-31; bentonite A of Elder, 1985), *N. juddii* (90-O-19 and 90-O-49; bentonite B of Elder, 1985), *W. devonense* (90-O-33; bentonite C of Elder, 1985), and *P. flexuosum* (90-O-34; bentonite D of Elder, 1985) zones. We also collected new samples from these sites, as well as from the *N. juddii* and *W. devonense* zones in the GSSP at Pueblo, Colorado, for both sanidine and zircon dating (Table 1).

$^{40}Ar/^{39}Ar$ GEOCHRONOLOGY

From each sanidine sample between 33 and 103 laser fusion $^{40}Ar/^{39}Ar$ ages were determined on single or multicrystal aliquots at the University of Wisconsin–Madison (Table 1; Items DR1

*E-mail: smeyers@geology.wisc.edu.

[1]GSA Data Repository item 2012017, background information on the radioisotopic results and intercalibration techniques, is available online at www.geosociety.org/pubs/ft2012.htm, or on request from editing@geosociety.org or Documents Secretary, GSA, P.O. Box 9140, Boulder, CO 80301, USA.

TABLE 1. SUMMARY OF $^{206}Pb/^{238}U$ AND $^{40}Ar/^{39}Ar$ AGES, WITH ANALYTICAL UNCERTAINTIES AT 2σ OR THE 95% CONFIDENCE LEVEL (RESPECTIVELY), AND FULL RADIOISOTOPIC UNCERTAINTIES AT 2σ*

Biozone sample	Obradovich (1993)	UW–Madison $^{40}Ar/^{39}Ar$ fusion analyses									NIGL $^{206}Pb/^{238}U$ isotope analyses		
	TCs 28.32 Ma	Apparent ages FCs 28.02 Ma			Apparent ages FCs 28.305 Ma			Apparent ages FCs 28.201 Ma					
	Age (Ma ±95%)	Age (Ma)	±95%	±2σ	Age (Ma)	±95%	±2σ	Age (Ma)	±95%	±2σ	Age (Ma)	±2σ	±2σ
Pseudaspidoceras flexuosum													
90-O-34	93.40 ± 0.63	93.06	±0.21	±1.58	94.01	±0.21	±0.24	93.67	±0.21	±0.31			
AZLP-08–05											94.09	±0.13	±0.19
Watinoceras devonense													
AZLP-08–04		93.20	±0.33	±1.60	94.16	±0.33	±0.35	93.81	±0.33	±0.40	94.37	±0.04	±0.14
K-07–01C		93.22	±0.30	±1.61	94.17	±0.30	±0.33	93.83	±0.30	±0.38			
90-O-33	93.25 ± 0.55	93.15	±0.21	±1.58	94.10	±0.21	±0.25	93.76	±0.21	±0.31			
Weighted mean age:		93.18	±0.12	±1.57	94.14	±0.12	±0.17	93.79	±0.12	±0.26			
Neocardioceras juddii													
K-07–01B		93.45	±0.27	±1.60	94.41	±0.27	±0.29	94.07	±0.27	±0.36	94.44	±0.07	±0.15
NE-08–01		93.48	±0.37	±1.62	94.44	±0.37	±0.40	94.10	±0.37	±0.44	94.01	±0.04	±0.14
90-O-19	93.30 ± 0.40	93.45	±0.31	±1.60	94.41	±0.31	±0.33	94.07	±0.31	±0.39			
90-O-49	93.59 ± 0.58	93.53	±0.23	±1.59	94.49	±0.23	±0.27	94.15	±0.23	±0.33			
Weighted mean age:		93.48	±0.14	±1.58	94.44	±0.14	±0.18	94.10	±0.14	±0.27			
Euomphaloceras septemseriatum													
AZLP-08–02		93.49	±0.24	±1.59	94.45	±0.24	±0.27	94.11	±0.24	±0.34			
90-O-31	93.49 ± 0.89	93.63	±0.19	±1.59	94.59	±0.19	±0.23	94.25	±0.19	±0.30			
Weighted mean age:		93.58	±0.15	±1.58	94.54	±0.15	±0.20	94.20	±0.15	±0.28			
Vascoceras diartianum													
90-O-30	93.90 ± 0.72	93.81	±0.17	±1.59	94.77	±0.17	±0.21	94.43	±0.17	±0.29			
AZLP-08–01											94.28	±0.08	±0.15

Note: TCs—Taylor Creek sanidine; FCs—Fish Canyon sanidine; NIGL—Natural Environment Research Council Isotope Geoscience Laboratory; UW—University of Wisconsin.

*See Table DR4 (see footnote 1) for further information.

and DR2). Whereas the 2σ analytical uncertainty associated with each individual measurement is large, 0.7–2.0 m.y., and may mask complexities in the data, outliers (mainly analyses with <97% radiogenic Ar) are few (≤5% in most samples) and weighted mean ages have precisions of ~±0.3% (Table 1; Fig. 1). Notwithstanding, Gaussian distributions and weighted mean ages for a given bentonite sampled at different localities strongly suggest a common eruptive age, and thus correlation among bentonites that occur within a biozone (Fig. 1). Moreover, there is no detectable difference in age between legacy samples of Obradovich (1993) and the newly collected samples; consequently, we assume that bentonites from a given biozone are equivalent and have calculated weighted mean ages for these groups of results from bentonites in the *E. septemseriatum*, *N. juddii*, and *W. devonense* zones (Table 1). The relatively short duration of the study interval yields stratigraphically distinct ash beds with ages indistinguishable from one another, given the analytical uncertainties, indicating that the $^{40}Ar/^{39}Ar$ technique cannot resolve geologic events at the <1‰ level. This limitation is obviated by intercalibration with the astrochronology (see following). To facilitate comparison with the U-Pb results, we report weighted mean ages with analytical uncertainties at the 95% confidence level, along with the 2σ total uncertainty (analytical, ^{40}K decay constant, and Fish Canyon sanidine standard age contributions) using three proposed Fish Canyon sanidine ages: 28.02 Ma (Renne et al., 1998), 28.201 Ma (Kuiper et al., 2008), and 28.305 Ma (Renne et al., 2010; Table 1).

U-Pb GEOCHRONOLOGY

Using the EARTHTIME ^{205}Pb-^{233}U-^{235}U tracer solution (Condon et al., 2007) and the CA ID-TIMS method (Mattinson, 2005; Mundil et al., 2004), zircons (single crystals and fragments) from five samples, representing four of the five bentonites for which we report new $^{40}Ar/^{39}Ar$ data, were measured at the British Geological Survey Natural Environment Research Council Isotope Geoscience Laboratory using the procedures outlined in Item DR3.With three exceptions, each zircon gives a concordant $^{206}Pb/^{238}U$ and $^{207}Pb/^{235}U$ age, and since the former is more precise, it is used to determine the ages of the bentonites. Whereas the precision of each single crystal $^{206}Pb/^{238}U$ age of ~0.1% is a strength, samples yield $^{206}Pb/^{238}U$ ages that span 0.6 to older than 1.0 m.y., reflecting inheritance or recycling of some zircon during protracted evolution of the volcanic sources (Fig. 1). Thus, selection of which of the youngest zircons best estimates the eruptive age requires a choice as to whether chemical abrasion has eliminated all zircon affected by Pb loss, and which zircons to include in determining an eruption age.

Schoene et al. (2010) faced similar choices in determining the $^{206}Pb/^{238}U$ ages that most closely reflect time since deposition of four ash beds bracketing the Triassic-Jurassic boundary; in each case the youngest zircon, the age of which overlapped a group of several other crystals, was chosen, whereas significantly younger ages were excluded owing to Pb loss, and crystals as much as 3 m.y. older were excluded as inherited or recycled. Following this approach, we select the youngest group of zircons, those that may best reflect closed-system behavior of the U-Pb system, as our best estimate of the time since eruption and deposition. Zircons suspected of bias due to Pb loss, inheritance, or magmatic residence, have been excluded (Table 1; Fig. 1).

The resultant $^{206}Pb/^{238}U$ ages should agree with the stratigraphic order; i.e., with the oldest ash bed in the *V. diartianum* zone and the youngest in the *P. flexuosum* zone. On the condition that the *V. diartianum* $^{206}Pb/^{238}U$ age does not reflect residual Pb loss, sample NE-08–01 (*N. juddii* zone in Nebraska) is in stratigraphic order, whereas sample K-07–01B (*N. juddii* zone in Colorado) is not (Table 1). These results could call into question our assumption, based solely on the $^{40}Ar/^{40}Ar$ ages, that each bentonite sample site in a given biozone is correlative.

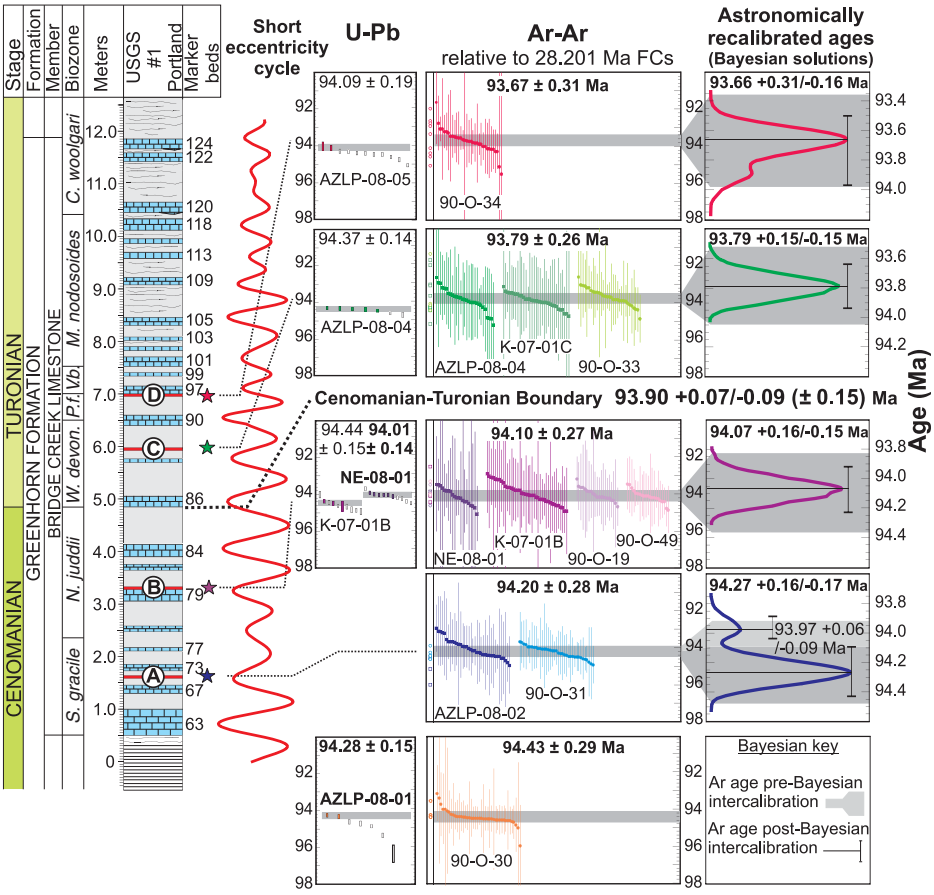

Figure 1. Lithostratigraphy and biostratigraphy of Bridge Creek Limestone Member in U.S. Geological Survey (USGS) #1 Portland Core (Sageman et al., 2006) (A–D: radioisotopically dated bentonites), with bandpass-filtered short-eccentricity cycle (using grayscale data from Meyers et al., 2001). Bandpassed record is provided for schematic purposes only; orbital time scale (OTS) was constructed via integration of sedimentation rate curve, derived via evolutive harmonic analysis (Item DR5 [see footnote 1]). $^{206}Pb/^{238}U$ and $^{40}Ar/^{39}Ar$ individual analyses are plotted with analytical uncertainties (2σ), and weighted mean ages, in bold, are reported with total uncertainties (2σ). Analyses excluded from weighted mean calculations for both $^{206}Pb/^{238}U$ (i.e., Pb loss; inheritance) and $^{40}Ar/^{39}Ar$ (i.e. <97% $^{40}Ar^*$; age outlier) are indicated by unfilled symbols. Bayesian $^{40}Ar/^{39}Ar$ solutions following intercalibration with OTS are shown using probability density plots (posterior marginal distributions) for each fully propagated $^{40}Ar/^{39}Ar$ age (this excludes lowermost bentonite corresponding to *Vascoceras diartianum* because it does not occur in USGS #1 Portland core). Bayesian $^{40}Ar/^{39}Ar$ ages incorporate ±20 k.y. uncertainty in OTS, and are reported with 95% credible intervals. Cenomanian-Turonian boundary age is calculated using Bayesian $^{40}Ar/^{39}Ar$ solutions and OTS, with analytical and total uncertainties. *S. gracile—Sciponoceras gracile*; *N. juddii—Neocardioceras juddii*; *W. devon.—Watinoceras devonense*; *V.b.—Vascoceras birchbyi*; *P.f.—Pseudaspidoceras flexuosum*; *M. nodosoides—Mammites nodosoides*; *C. woolgari—Collignoniceras woolgari*.

However, the astrochronologic model in Sageman et al. (2006) indicates that the duration of the *N. juddii* zone is 300 k.y., whereas the two sets of U-Pb data, when compared using only the analytical uncertainties, give ages of 94.44 ± 0.07 and 94.01 ± 0.04 Ma that differ by at least 320 k.y. at the 2σ level. Therefore, we suspect that the K-07–01B sample contains a large proportion of inherited zircons that do not reflect the time since eruption, and we take the U-Pb age from Nebraska as the most accurate estimate of time since eruption.

Provided that the above interpretation is correct, the youngest zircons from bentonites in the *W. devonense* and *P. flexuosum* zones are older than the zircons found in the *N. juddii* zone at site NE-08–01 (Fig. 1), thereby violating the law of superposition, and suggesting that all zircons in samples AZLP-08–04 and AZLP-08–05 are inherited or recycled and thus do not reflect the time since eruption (Item DR3), and therefore cannot be used to calibrate the $^{40}Ar/^{39}Ar$ system. Alternatively, the $^{206}Pb/^{238}U$ weighted mean ages of AZLP-08–01 and NE-08–01 reflect residual Pb loss. Consequently, the $^{206}Pb/^{238}U$ ages of K-07–01B, AZLP-08–04, and AZLP-08–05 do not violate stratigraphic order, and thus would not be interpreted to reflect inheritance.

SUMMARY OF RADIOISOTOPIC GEOCHRONOLOGY

Regardless of which Fish Canyon sanidine age is used, the weighted mean $^{40}Ar/^{39}Ar$ ages of the five bentonites obey stratigraphic superposition, and the relative time differences between samples are consistent with the astrochronologic age model (Fig. DR3). In contrast, the $^{206}Pb/^{238}U$ data are more complex, with intrasample variation in zircon ages and defiance of stratigraphic superposition. Due to the high closure temperature for U-Pb in zircon, such dispersion in ages for individual zircons from volcanic-magmatic systems can reflect processes that predate eruption and/or the inclusion of xenocrystic material. Younger U-Pb ages are possibly the result of postcrystallization Pb loss; however, with development of the CA ID-TIMS method (Mattinson, 2005), the occurrence of U-Pb ages thought to record Pb loss has been greatly reduced. Notwithstanding, most high-precision CA ID-TIMS U-Pb data sets contain a small number (<5%) of analyses that are considered to reflect Pb loss (e.g., Davydov et al., 2010; Schoene et al., 2010). Our data set is no different, and we exclude 3 of 47 individual U-Pb ages due to suspected Pb loss.

The alternative interpretation that the U-Pb ages of the three youngest bentonites (K-07–01B, AZLP-08–04, and AZLP-08–05) agree with the corresponding $^{40}Ar/^{39}Ar$ ages, provided the latter are calculated using a 28.305 Ma Fish Canyon sanidine age (Table 1), would require that the coherent zircon U-Pb data from NE-08–1 is ~400 k.y. too young due to Pb loss. However, it is the experience of the U-Pb community (e.g., Davydov et al., 2010; Schoene et al., 2010) that Pb loss does not manifest as coherent populations. Moreover, it would require that the sanidine crystals in samples NE-08–1 and AZLP-08–1 are older than the zircons. While it is reasonable for zircon U-Pb ages to be older than sanidine $^{40}Ar/^{39}Ar$ ages in an erupted magma, the converse is not permissible given the higher closure temperature of zircon relative to sanidine. Thus it is difficult to reconcile the 28.305 Ma calibration of Fish Canyon sanidine with our results.

UNITING CTB RADIOISOTOPIC AND ASTROCHRONOLOGIC DATA TO DERIVE A NEW TIME SCALE

Whereas the $^{40}Ar/^{39}Ar$ data provide an age with a well-defined uncertainty for each bentonite (Fig. 1), the floating astrochronology for the CTB GSSP (Meyers et al., 2001; Sageman et al., 2006) yields a more highly resolved estimate of the duration between stratigraphic horizons. We employ two statistical approaches to unite these sources of geochronologic information, using the four radioisotopically dated bentonites (A, B, C, and D in Fig. 1) that can be precisely located within the astronomically tuned stratigraphy. The first technique utilizes

the orbitally derived duration between each dated bentonite and the CTB to provide four statistically independent estimates of the boundary age. The weighted mean of these estimates indicates a CTB age of 93.89 Ma ± 0.07 Ma (2σ analytical uncertainty), or 93.89 Ma ± 0.14 Ma (2σ total radioisotopic uncertainty).

The second technique uses Bayesian analysis as a quantitative framework for objectively integrating the two sources of geochronologic information (Buck et al., 1992). This approach yields a time scale that is statistically compatible with the astrochronologic and radioisotopic data, while also permitting an explicit astronomical recalibration of the radioisotopic ages (see Item DR5), thereby representing a powerful innovation. We implement the Bayesian intercalibration using Markov Chain Monte Carlo simulations; the radioisotopic ages of each bentonite are linked (Markov Chain) by the orbital time scale, and random sampling of each $^{40}Ar/^{39}Ar$ probability density (Monte Carlo) is conducted, with the rejection of ages that violate astrochronologic and radioisotopic constraints.

A second important innovation of this Bayesian approach is the explicit consideration of potential orbital time scale uncertainties (tolerances). We investigate a range of plausible uncertainties, varying in magnitude from ±10 k.y. to ±50 k.y. for the duration between individual radioisotopically dated bentonites. This approach allows for uncertainty in the short eccentricity tuning frequency (Meyers et al., 2001), and potential hiatus (Meyers and Sageman, 2004).

Bayesian intercalibration, when executed using the analytical $^{40}Ar/^{39}Ar$ age uncertainties, is insensitive to the range of investigated orbital time scale tolerances (Item DR5). In contrast, intercalibration using the total $^{40}Ar/^{39}Ar$ age uncertainties demonstrates a degree of instability (with the ages of individual bentonites varying by as much as 140 k.y.), particularly at low tolerances (<15 k.y.; Item DR5). The astronomically recalibrated ages in Figure 1 utilize an intermediate tolerance of ±20 k.y. Ages recalibrated using the analytical uncertainties can achieve permil level of resolution, whereas those recalibrated using the total uncertainties can be constrained to better than 2‰.

Utilizing the Bayesian-anchored astrochronology, the age of the CTB is estimated to be 93.90 +0.07/–0.09 Ma (95% credible interval, a Bayesian confidence interval; analytical and orbital time scale uncertainty), or 93.90 ± 0.15 Ma (95% credible interval; total radioisotopic and orbital time scale uncertainty). These results shift the previously determined age of 93.55 ± 0.50 Ma (Gradstein et al., 2004; reported with analytical uncertainty only; total uncertainty is >1.5 m.y.) by +0.37%, with nearly an order of magnitude improvement in precision. Our results agree with the astronomically interpolated CTB age of 94.12 ± 0.28 Ma proposed by Barker et al. (2011), based on $^{206}Pb/^{238}U$ dating of an ash bed below the boundary. Moreover, a duration of 27.94 ± 0.16 Ma can be calculated between the new CTB age and the Cretaceous-Paleogene boundary age of 65.96 ± 0.04 Ma (Kuiper et al., 2008), with an uncertainty of less than half of a 405 k.y. eccentricity cycle. Our findings thereby provide a means for quantitative evaluation of future Late Cretaceous astronomical time scales, and yield an important constraint for solar system dynamic modeling (Laskar et al., 2004).

ACKNOWLEDGMENTS

This work was supported by U.S. National Science Foundation grant EAR-0959108 (Meyers, Singer, Sageman), the University of Wisconsin–Madison Vilas Trust (Singer), and a Shell Oil Undergraduate grant (Siewert). We thank KC McKinney, B. Cobban, and N. Heim for assistance with field work. L. Hinnov and three anonymous referees provided helpful reviews.

REFERENCES CITED

Barker, I.R., Moser, D.E., Kamo, S.L., and Plint, A.G., 2011, High-precision U-Pb zircon ID-TIMS dating of two regionally-extensive bentonites: Cenomanian stage, Western Canada Foreland Basin: Canadian Journal of Earth Sciences, v. 48, p. 543–556, doi:10.1139/E10-042.

Buck, C.E., Litton, C.D., and Smith, A.F.M., 1992, Calibration of radiocarbon results pertaining to related archaeological events: Journal of Archaeological Science, v. 19, p. 497–512, doi:10.1016/0305-4403(92)90025-X.

Cobban, W.A., Walaszczyk, I., Obradovich, J.D., and McKinney, K.C., 2006, A USGS zonal table for the Upper Cretaceous middle Cenomanian-Maastrichtian of the Western Interior of the United States based on ammonites, inoceramids, and radiometric ages: U.S. Geological Survey Open-File Report 2006–1250, 46 p.

Condon, D., Schoene, B., Bowring, S.A., Parrish, R., McLean, N., Noble, S., and Crowley, Q., 2007, EARTHTIME: Isotopic tracers and optimized solutions for high-precision U-Pb ID-TIMS geochronology: Eos (Transactions, American Geophysical Union), v. 88, no. 52, abs. V41E–06.

Crowley, J.L., Schoene, B., and Bowring, S.A., 2007, U-Pb dating of zircon in the Bishop Tuff at the millennial scale: Geology, v. 35, p. 1123–1126, doi:10.1130/G24017A.1.

Davydov, V.I., Crowley, J.L., Schmitz, M.D., and Poletaev, V.I., 2010, High-precision U-Pb zircon age calibration of the global Carboniferous time scale and Milankovitch band cyclicity in the Donets Basin, eastern Ukraine: Geochemistry, Geophysics, Geosystems, v. 11, Q0AA04, doi:10.1029/2009GC002736.

Elder, W.P., 1985, Biotic patterns across the Cenomanian-Turonian extinction boundary near Pueblo, Colorado, *in* Pratt, L.M., et al., eds., Fine-grained deposits and biofacies of the Cretaceous Western Interior Seaway: Evidence of cyclic sedimentary processes: Field Trip Guidebook 4: Tulsa, Society of Economic Paleontologists and Mineralogists, p. 157–169.

Elder, W.P., 1987, Cenomanian-Turonian (Cretaceous) stage boundary extinctions in the Western Interior of the United States [Ph.D. thesis]: Boulder, Colorado, University of Colorado, 621 p.

Elder, W.P., 1991, Molluscan paleoecology and sedimentation patterns of the Cenomanian-Turonian extinction interval in the southern Colorado Plateau region, *in* Nations, J.D., and Eaton, J.G., eds., Stratigraphy, depositional environments, and sedimentary tectonics of the western margin, Cretaceous Western Interior Seaway: Geological Society of America Special Paper 260, p. 113–137.

Gradstein, F.M., Ogg, J.G., and Smith, A.G., 2004, A geologic time scale 2004: Cambridge, Cambridge University Press, 610 p.

Kennedy, W.J., Walaszczyk, I., and Cobban, W.A., 2005, The Global Boundary Stratotype Section and Point for the base of the Turonian Stage of the Cretaceous; Pueblo, Colorado, U.S.A.: Episodes, v. 28, no. 2, p. 93–104.

Kirkland, J.I., 1991, Lithostratigraphic and biostratigraphic framework for the Mancos Shale (late Cenomanian to middle Turonian) at Black Mesa, northeastern Arizona, *in* Nations, J.D., and Eaton, J.G., eds., Stratigraphy, depositional environments, and sedimentary tectonics of the western margin, Cretaceous Western Interior Seaway: Geological Society of America Special Paper 260, p. 85–111.

Kuiper, K.F., Deino, A., Hilgen, F.J., Krijgsman, W., Renne, P.R., and Wijbrans, J.R., 2008, Synchronizing rock clocks of Earth history: Science, v. 320, p. 500–504, doi:10.1126/science.1154339.

Laskar, J., Robutel, P., Joutel, F., Gastineau, M., Correia, A.C.M., and Levrard, B., 2004, A long-term numerical solution for the insolation quantities of the Earth: Astronomy and Astrophysics, v. 428, p. 261–285, doi:10.1051/0004-6361:20041335.

Mattinson, J.M., 2005, Zircon U/Pb chemical abrasion (CA-TIMS) method: Combined annealing and multi-step partial dissolution analysis for improved precision and accuracy of zircon ages: Chemical Geology, v. 220, p. 47–66, doi:10.1016/j.chemgeo.2005.03.011.

Meyers, S.R., and Sageman, B.B., 2004, Detection, quantification, and significance of hiatuses in pelagic and hemipelagic strata: Earth and Planetary Science Letters, v. 224, p. 55–72, doi:10.1016/j.epsl.2004.05.003.

Meyers, S.R., Sageman, B., and Hinnov, L., 2001, Integrated quantitative stratigraphy of the Cenomanian-Turonian Bridge Creek Limestone Member using evolutive harmonic analysis and stratigraphic modeling: Journal of Sedimentary Research, v. 71, p. 628–643, doi:10.1306/012401710628.

Mundil, R., Ludwig, K.R., Metcalfe, I., and Renne, P.R., 2004, Age and timing of the Permian mass extinctions: U/Pb dating of closed-system zircons: Science, v. 305, no. 5691, p. 1760–1763, doi:10.1126/science.1101012.

Obradovich, J., 1993, A Cretaceous time scale, *in* Caldwell, W.G.E., and Kauffman, E.G., eds., Evolution of the Western Interior Basin: Geological Society of Canada Special Paper 39, p. 379–396.

Renne, P.R., Swisher, C.C., III, Deino, A.L., Kamer, D.B., Owens, T.L., and DePaolo, D.J., 1998, Intercalibration of standards, absolute ages, and uncertainties in $^{40}Ar/^{39}Ar$ dating: Chemical Geology, v. 145, p. 117–152, doi:10.1016/S0009-2541(97)00159-9.

Renne, P.R., Mundil, R., Balco, G., Min, K., and Ludwig, K.R., 2010, Joint determination of ^{40}K decay constants and $^{40}Ar^*/^{40}K$ for the Fish Canyon sanidine standard, and improved accuracy for $^{40}Ar/^{39}Ar$ geochronology: Geochimica et Cosmochimica Acta, v. 74, p. 5349–5367, doi:10.1016/j.gca.2010.06.017.

Sageman, B.B., Rich, J., Arthur, M.A., Birchfield, G.E., and Dean, W.E., 1997, Evidence for Milankovitch periodicities in Cenomanian-Turonian lithologic and geochemical cycles, Western Interior, U.S.: Journal of Sedimentary Research, v. 67, p. 286–301, doi:10.1306/D4268554-2B26-11D7-8648000102C1865D.

Sageman, B.B., Meyers, S.R., and Arthur, M.A., 2006, Orbital time scale and new C-isotope record for Cenomanian-Turonian boundary stratotype: Geology, v. 34, p. 125–128, doi:10.1130/G22074.1.

Schoene, B., Guex, J., Bartolini, A., Schaltegger, U., and Blackburn, T.J., 2010, Correlating the end-Triassic mass extinction and flood basalt volcanism at the 100 ka level: Geology, v. 38, p. 387–390, doi:10.1130/G30683.1.

Manuscript received 17 March 2011
Revised manuscript received 3 August 2011
Manuscript accepted 10 August 2011

Printed in USA